Check for updates

The Journal of Phytopharmacology 2026; 15(2):164-175
Online at: www.phytopharmajournal.com

The Journal of Phytopharmacology
(Pharmacognosy and phytomedicine Research)

Research Article

ISSN 2320-480X
JPHYTO 2026; 15(2): 164-175
March- April
Received: 14-11-2025
Accepted: 21-04-2026
Published: 27-04-2026

doi: 10.31254/phyto.2026.15207

In silico molecular docking evaluation of phytochemicals from Siddha medicinal plants as potential inhibitors of snake venom phospholipase A_2

Chenthamarai Selvi Ganesan, Shanmugam Muthu

Chenthamarai Selvi Ganesan
Assistant Professor, Department of Toxicology, Govt. Siddha Medical College, Palayamkottai, Tirunelveli - 627002, Tamil Nadu, India

Shanmugam Muthu
PG Scholar, Department of Toxicology, Govt. Siddha Medical College, Palayamkottai, Tirunelveli - 627002, Tamil Nadu, India

ABSTRACT

Background: Snakebite envenomation remains a neglected tropical disease with significant global morbidity. Phospholipase A_2 (PLA_2) is a venom enzyme that causes inflammation, tissue destruction and myonecrosis. Siddha medicinal plants offer promising phytochemical compounds for novel antivenom therapeutics. **Objective:** To evaluate selected phytochemicals from Siddha medicinal plants as potential inhibitors of snake venom phospholipase A_2 using drug-likeness screening, ADMET profiling, and molecular docking approaches. **Methods:** Nine phytocompounds from Siddha herbs, Indigotin, Aristolochic acid, Lucidenic acid, Esculetin, Leucasperoside B, Friedelin, Rutin, Quercetin, and Beta-sitosterol, were evaluated through drug-likeness screening (Lipinski's Ro5, Ghose, Veber, Egan rules), *in silico* ADMET profiling (SwissADME, pkCSM), and molecular docking against PLA_2 (PDB: 2QOG) using AutoDock 4.2. **Results:** Binding affinities ranged from -5.62 kcal/mol (Indigotin) to -12.73 kcal/mol (Rutin). Rutin showed the strongest binding, while Quercetin and Lucidenic acid exhibited the best balance of drug-likeness, ADMET properties, and catalytic site engagement (Asp49, Tyr52). Seven compounds directly interacted with core catalytic residues. **Conclusion:** This first systematic *in silico* study of Siddha phytocompounds against snake venom PLA_2 identifies Quercetin and Lucidenic acid as priority lead candidates, providing computational rationale for traditional antivenom use and a foundation for future experimental validation.

Keywords: Siddha Medicine, Snake Venom, Phospholipase A_2, Molecular Docking, Antivenom, Phytochemicals.

INTRODUCTION

Snakebite envenomation is a critical, neglected tropical disease, causing significant global morbidity and mortality [1]. A key pathogenic component is phospholipase A_2 (PLA_2), an enzyme that hydrolyzes membrane phospholipids, triggering a cascade of inflammatory events leading to local tissue damage, myonecrosis, and systemic toxicity [2,3]. The catalytic activity of PLA_2 is mediated by a conserved active site containing residues such as His48, Asp49, and Tyr52 [4]. Current antivenom therapies, which are polyclonal antisera, have significant limitations, including high cost, risk of adverse reactions, and limited efficacy against local tissue damage [5], necessitating new therapeutic strategies. Medicinal plants have been a traditional source of antidotes for snakebites in various cultures [6]. In particular, Siddha medicine has used specific medicinal herbs to neutralize venom. This research looks at nine phytochemicals found in Siddha medicinal plants, including Indigifera tinctoria, Aristolochia bracteolate, Rhinacanthus communis, Leucas aspera, Aristolochia indica, Hemidesmus indicus, Musa paradisiaca, and Carollocarpus epigaeus. This study focuses on Indigotin, Aristolochic acid, Lucidenic acid, Esculetin, Leucasperoside B, Friedelin, Rutin, Quercetin, and Beta-sitosterol, from these medicinal herbs [7]. The selection of *Corallocarpus epigaeus*, *Leucas aspera*, *Musa paradisiaca*, *Rhinocanthus communis*, *Aristolochia bracteolata*, and *Aristolochia indica* for molecular docking analyses is based on their prevalent use in Siddha medicine to treat snake bites. These plants are recognized for various phytochemicals, including flavonoids, alkaloids, terpenoids, and aristolochic acids, which are associated with antivenom properties. Prior studies in ethnopharmacology and laboratory experiments suggest that these compounds may inhibit key snake venom enzymes such as phospholipase A_2, proteases, and hyaluronidases, thereby diminishing the venom's toxic effects [8-13]. *Indigofera tinctoria* has impressive antidote properties.

Correspondence:
Dr. Chenthamarai Selvi Ganesan
Assistant Professor, Department of Toxicology, Govt. Siddha Medical College, Palayamkottai, Tirunelveli - 627002, Tamil Nadu, India
Email: chenthamaraianand@gmail.com

Its phytochemicals show antioxidant, anti-inflammatory, and toxin-neutralizing effects. It might affect oxidative stress pathways, reduce cellular damage, and improve detoxification processes. This supports its effectiveness in dealing with various toxic exposures [14]. The methanolic root extract of *Hemidesmus indicus* effectively reduced the lethal effects, bleeding, and clotting problems caused by the venom of *Vipera russellii* in animal studies. It worked better than *Pluchea indica*, highlighting its strong potential as an antivenom without needing immunoprecipitation. This suggests that the active phytochemicals mediate the inhibition of toxins [15]. Using molecular docking, an established computational method for rapid screening of bioactive compounds [16], we evaluated the inhibitory potential of these phytocomponents against PLA_2 (PDB ID: 2QOG). The objective was to determine their binding affinity and interactions with the enzyme's catalytic residues, thereby providing a scientific basis for their traditional use and identifying promising candidates for novel anti-venom therapeutics.

MATERIAL AND METHODS

Phospholipases A2

Snake venom Phospholipase A2 (PLA2, PDB 2QOG) is a key toxin causing tissue destruction (myotoxicity) and swelling (oedema). Xiao H *et al*. highlight PLA2 as a conserved and abundant component across many snake species, making it a strong candidate for broad-spectrum antivenom development [17]. Its function depends on a specific active site with core amino acids His48, Asp99, Lys49, and Tyr52. These residues are responsible for catalyzing the breakdown of cell membrane phospholipids. Inhibiting this enzyme is a strategic anti-venom approach. A potent inhibitor, such as a phytocomponent, would bind precisely to these core amino acids, forming hydrogen bonds. This action physically blocks the enzyme's hydrophobic channel, preventing the binding of its phospholipid substrate. Consequently, the release of pro-inflammatory fatty acids is halted, stopping the toxin's allosteric activation and its damaging effects. By occupying this active site, such an inhibitor can neutralize this venom component, making it a promising therapeutic candidate for snakebite management.

PDB	Name of the Target
2QOG	Phospholipases A2

Figure 1: 3D- Structure of Phospholipases A2 (PDB) - 2QOG

Selection of Ligands and Protein Preparation

A selection of nine phytocomponents was made from different medicinal herbs, chosen for their known pharmacological effects. Table 1 contains a list of the herbs and their associated compounds. [18-20]. The three-dimensional crystal structure of the target enzyme, Phospholipase A_2 (PDB ID: 2QOG), was obtained from the Protein Data Bank (www.rcsb.org). To prepare the protein structure for docking, water molecules and co-crystallized ligands were taken out, and then polar hydrogen atoms and Kollman united atom charges were added using AutoDock Tools [21].

Ligand Preparation

The 2D representations of the chosen phytochemicals were created and transitioned into 3D models. Energy minimization was conducted utilizing the MMFF94 force field. Gasteiger charges were applied, and torsional bonds were established to ensure the ligands were flexible for docking simulations.

Drug likeness and ADMET Analysis

Assessing drug likeness and conducting ADMET analysis occur before molecular docking. This process helps filter out compounds with the right pharmacokinetic and safety characteristics. Drug likeness is typically evaluated using Lipinski's Rule of Five. This rule considers molecular weight, lipophilicity, and hydrogen bonding features to estimate oral bioavailability. ADMET parameters, which include absorption, distribution, metabolism, excretion, and toxicity, can be predicted using tools like SwissADME and pkCSM. This approach helps prioritize lead compounds, improves docking accuracy, and reduces the likelihood of failures in the later stages of drug development. [22-24].

Molecular Docking Studies

Molecular docking studies were conducted utilizing AutoDock 4.2 [21]. A grid box measuring 60 × 60 × 60 Å with a grid spacing of 0.375 Å was positioned over the active site of PLA_2 to cover the critical residues (His48, Asp49, Tyr52, Asp99). The Lamarckian Genetic Algorithm (LGA) was used to search for different conformations. The docking parameters were configured for a maximum of 250,000 energy evaluations and a population size of 150. Ten separate docking runs were carried out for each ligand. The resulting conformations were grouped based on root-mean-square deviation (RMSD), and the conformation with the most favourable (lowest) free energy of binding was chosen for further analysis.

Analysis of Docking Results

The binding affinity (estimated free energy of binding, ΔG in kcal/mol), estimated inhibition constant (Ki), and the nature of interactions (hydrogen bonds, hydrophobic, electrostatic) between the ligands and the amino acid residues of PLA_2 were analyzed. The visualization of protein-ligand complexes was carried out to identify specific residue interactions.

RESULTS

Phytocomponents Selected for docking-

Ligand Properties

The molecular properties of the nine phytocomponents, including molecular weight, formula, and key physicochemical descriptors relevant to drug-likeness (hydrogen bond donors/acceptors, rotatable bonds), are summarized in Table 1.

Drug-likeness

Drug likeness was evaluated using SwissADME [23]. Lipinski's rule of 5, Ghose rule, Veber rule, Egan rule and weighted quantitative estimate of drug-likeness score were used as criteria to evaluate the effectiveness of the selected phytocomponents. Lipinski's Rule of Five is widely adopted for predicting oral bioavailability, stipulating that drug-like molecules should have a molecular weight ≤ 500 Da, a calculated octanol–water partition coefficient (MLogP) ≤ 4.15, no more than five hydrogen bond donors, and no more than ten hydrogen bond acceptors [22] Compounds violating more than one criterion are considered poor candidates for oral administration. Indigotin, Aristolochic acid, Lucidenic acid, Esculetin, and Quercetin displayed zero violations of Lipinski's Ro5. Friedelin and Beta-sitosterol each unveiled one violation. In contrast, Leucasperoside B and Rutin show three violations each and consequently failed the Ro5 filter.

The Ghose filter extends Lipinski's framework by including the calculated log P (−0.4 to +5.6), molecular weight (160–480 Da), molar refractivity (40–130), and total atom count (20–70) [33]. It is considered more exacting and is often employed to define the boundaries of drug-like chemical space. Indigotin, Aristolochic acid, and Quercetin passed the Ghose filter without any violations.

Lucidenic acid and Esculetin each displayed one violation. Friedelin and Beta-sitosterol exhibited two violations, reflecting their higher lipophilicity and molecular size. Leucasperoside B and Rutin failed the Ghose filter with four violations each, consistent with their large, polar, and heavily hydroxylated structures typical of flavonoid glycosides.

The Veber rule predicts oral bioavailability based on molecular flexibility and polarity, requiring that a compound possess ≤ 10 rotatable bonds and a polar surface area (PSA) of ≤ 140 Å², parameters closely correlated with intestinal permeability [34]. Indigotin, Aristolochic acid, Lucidenic acid, Esculetin, Friedelin, Quercetin, and Beta-sitosterol - passed the Veber rule, showing acceptable rotatable bond counts and polar surface areas. Leucasperoside B and Rutin failed, attributable to their excessive polar surface areas and high rotatable bond counts. The Egan rule assesses passive intestinal absorption based on two key descriptors: the polar surface area (PSA ≤ 131.6 Å²) and the calculated logarithm of the partition coefficient (AlogP98 ≤ 5.88) [35].

This model is based on experimental data from Caco-2 permeability studies and human intestinal absorption, offering a prediction of membrane permeability that is more closely aligned with biological reality. Indigotin, Aristolochic acid, Lucidenic acid, Esculetin, and Quercetin - passed the Egan rule, suggesting favourable absorption characteristics. Friedelin and Beta-sitosterol failed, likely due to their elevated lipophilicity Leucasperoside B and Rutin also failed. The QEDw (weighted quantitative estimate of drug-likeness) is a composite scoring metric that integrates eight physicochemical properties - molecular weight, lipophilicity (AlogP), hydrogen bond donors, hydrogen bond acceptors, polar surface area, number of rotatable bonds, presence of aromatic rings, and the absence of undesirable structural alerts [36]. Indigotin achieved the highest QEDw score of 0.72, indicating a strong overall drug-like profile Lucidenic acid (0.56) and Esculetin (0.55) also showed moderately good scores. Aristolochic acid (0.44), Beta-sitosterol (0.44), and Quercetin (0.43) exhibited intermediate QEDw values, suggesting partial drug-likeness. Friedelin recorded a score of 0.38. Leucasperoside B (0.17) and Rutin (0.14) demonstrated the lowest QEDw scores. These findings guide the prioritization of compounds for further pharmacokinetic and molecular docking studies.

ADMET analysis

In silico ADMET profiling shows clear differences in pharmacokinetics among the nine phytocompounds. Indigotin stands out as the most versatile compound, with high gastrointestinal absorption, unique blood-brain barrier permeability, and no P-gp efflux risk. However, its multi-CYP inhibitory activity raises concerns in polypharmacy situations. Esculetin and Lucidenic acid have favourable absorption profiles with limited metabolic risks, making them safer candidates for further development. Quercetin has high gastrointestinal absorption and well-documented bioactivity, but it poses significant CYP inhibition risks.

Aristolochic acid also has high gastrointestinal absorption, but it carries nephrotoxic risks noted in existing literature and inhibits several CYP isoforms, which raises major safety issues that may hinder its therapeutic development. Leucasperoside B and Rutin show consistently poor absorption and low skin permeation, limiting their use through standard oral or topical methods. Friedelin and Beta-Sitosterol have good skin permeation due to their lipophilic nature, but they display low gastrointestinal absorption. These findings create a solid pharmacokinetic framework to help prioritise phytocompounds for the next *in vitro* and *in vivo* validation studies.

Docking Analysis and Binding Affinity

The results from molecular docking indicated that all nine phytocomponents successfully interacted with the active site of PLA_2, showing noteworthy binding affinities as shown in Table 2. Rutin displayed the strongest binding, with a calculated free energy of binding of -12.73 kcal/mol and an exceptionally low inhibition constant (Ki) of 465.23 pM. Leucasperoside B also demonstrated a strong binding affinity of -9.77 kcal/mol (Ki = 68.74 nM). The remaining compounds, such as Beta-sitosterol (-7.69 kcal/mol), Lucidenic acid (-7.57 kcal/mol), Friedelin (-7.53 kcal/mol), and Aristolochic acid (-7.29 kcal/mol), exhibited significant binding potentials, with Ki values in the low micromolar range.

Analysis of Protein-Ligand Interactions

A critical analysis of the binding modes showed that most compounds interacted directly with the core catalytic residues of PLA_2. As summarized in Table 3, seven out of nine compounds - Indigotin, Aristolochic acid, Lucidenic acid, Leucasperoside B, Friedelin, Rutin, and Beta-sitosterol - formed significant interactions with residues such as Asp49 and Tyr52. These residues are part of the conserved active site and the hydrophobic channel. Notably, Rutin, despite its large size, formed a stable complex involving key residues Leu2, Trp31, Asp49, Tyr52, Asn67, and Trp70. Esculetin interacted with a different set of peripheral residues (Phe5, Asn6, Ile9, Ala18, Val19, Tyr22, Ala23, Trp31, Cys45, Leu106), while Quercetin interacted with Ser1, Leu2, Trp31, Tyr52, Asn67, and Trp70.

Table 1: List of Herbal Phytocomponents [25-32]

Herbs	Phytochemicals
Indigifera tinctoria	Indigotin
Aristolochia bracteolata	Aristolochic acid
Rhinacanthus communis	Lucidenic acid Esculetin
Leucas aspera	Leucasperoside B
Aristolochia indica	Friedelin
Hemidesmus indicus	Rutin
Musa paradisiaca	Quercetin
Carollocarpus epigaeus	Beta-sitosterol

Table 2: Ligand Properties of the Compounds Selected for Docking Analysis

Compound	Molar weight g/mol	Molecular Formula	H Bond Donor	H Bond Acceptor	Rotatable bonds
Indigotin	262.26 g/mol	$C_{16}H_{10}N_2O_2$	2	3	1
Aristolochic acid	341.27 g/mol	$C_{17}H_{11}NO_7$	1	7	2
Lucidenic acid	460.6 g/mol	$C_{27}H_{40}O_6$	3	6	4
Esculetin	178.14 g/mol	$C_9H_6O_4$	2	4	0
Leucasperoside B	626.7 g/mol2	$C_{32}H_{50}O_{12}$	7	12	7
Friedelin	426.7 g/mol	$C_{30}H_{50}O$	0	1	0
Rutin	610.5 g/mol	$C_{27}H_{30}O_{16}$	10	16	6
Quercetin	302.23 g/mol	$C_{15}H_{10}O_7$	5	7	1
β-sitosterol	414.7g/mol	$C_{29}H_{50}O$	1	1	6

Table 3: Drug-likeness evaluation of selected phytocompounds based on Lipinski's Ro5, Ghose filter, Veber rule, Egan rule, and QEDw score using SwissADME

Phytocompound name	Number of Lipinski's rule of violations	Lipinski's rule of 5	Number of Ghose rule violations	Ghose rule	Veber rule	Egan rule	Weighted quantitative estimate of drug-likeness (QEDw) score
Indigotin	0	Passed	0	Passed	Passed	Passed	0.72
Aristolochic acid	0	Passed	0	Passed	Passed	Passed	0.44
Lucidenic acid	0	Passed	1	Failed	Passed	Passed	0.56
Esculetin	0	Passed	1	Failed	Passed	Passed	0.55
Leucasperoside B	3	Failed	4	Failed	Failed	Failed	0.17
Friedelin	1	Passed	2	Failed	Passed	Failed	0.38
Rutin	3	Failed	4	Failed	Failed	Failed	0.14
Quercetin	0	Passed	0	Passed	Passed	Passed	0.43
Beta-sitosterol	1	Passed	2	Failed	Passed	Failed	0.44

Table 4: *In silico* ADMET properties of selected phytocompounds predicted using SwissADME, pkCSM, and admetSAR 2.0

Compound name	Indigotin	Aristolochic acid	Lucidenic acid	Esculetin	Leucasperoside B	Freiedlin	Rutin	Quercetin	Beta-Sitosterol
Skin Permeation Value (log Kp) cm/s	-5.96 cm/s	-5.85 cm/s	-7.41 cm/s	-6.52 cm/s	-9.14 cm/s	-1.94 cm/s	-10.26 cm/s	-7.05 cm/s	-2.20 cm/s
GI Absorption	High	High	High	High	Low	Low	Low	High	Low
BBB Permeability	Yes	No	No	No	No	No	No	No	No
P-gp Substrate	No	No	Yes	No	No	No	Yes	No	No
CYP1A2 Inhibitor	Yes	Yes	No	Yes	No	No	No	Yes	No
CYP2C19 Inhibitor	No	Yes	No	No	No	No	No	No	No
CYP2C9 Inhibitor	No	Yes	No	No	No	No	No	No	No
CYP2D6 Inhibitor	Yes	No	No	No	No	No	No	Yes	No
CYP3A4 Inhibitor	Yes	No	Yes	No	No	No	No	Yes	No

Table 5: Molecular docking studies of compounds against Phospholipases A2 (PDB) - 2QOG

Compounds	Est. Free Energy of Binding	Est. Inhibition Constant, Ki	Electrostatic Energy	Total Intermolec. Energy	Interact. Surface
Indigotin	-5.62 kcal/mol	76.04 uM	-0.05 kcal/mol	-5.62 kcal/mol	482.496
Aristolochic acid	-7.29 kcal/mol	4.51 uM	-1.20 kcal/mol	-8.31 kcal/mol	553.989
Lucidenic acid	-7.57 kcal/mol	2.85 uM	-1.23 kcal/mol	-8.29 kcal/mol	640.892
Esculetin	-6.06 kcal/mol	36.11 uM	-0.22 kcal/mol	-5.42 kcal/mol	441.858
Leucasperoside B	-9.77 kcal/mol	68.74 nM	-0.51 kcal/mol	-10.12 kcal/mol	783.37
Friedelin	-7.53 kcal/mol	3.02 uM	-0.05 kcal/mol	-7.53 kcal/mol	591.046
Rutin	-12.73 kcal/mol	465.23 pM	-0.39 kcal/mol	-7.07 kcal/mol	716.79
Quercetin	-7.02 kcal/mol	7.15 uM	-0.98 kcal/mol	-6.19 kcal/mol	499.466
Beta-sitosterol	-7.69 kcal/mol	2.29 uM	-0.02 kcal/mol	-9.37 kcal/mol	664.305

Table 6: Amino acid Residue Interaction of Lead against Phospholipases A2 (PDB) - 2QOG

Compounds	Interactions	Amino acid Residues									
Indigotin	2	31	49	52	67	70					
		TRP	ASP	TYR	ASN	TRP					
Aristolochic acid	2	01	02	31	49	52	67	70			
		SER	LEU	TRP	ASP	TYR	ASN	TRP			
Lucidenic acid	2	01	02	31	49	52	70	133			
		SER	LEU	TRP	ASP	TYR	TRP	CYS			
Esculetin	0	05	06	09	18	19	22	23	31	45	106
		PHE	ASN	ILE	ALA	VAL	TYR	ALA	TRP	CYS	LEU
Leucasperoside B	2	02	31	49	52	67	70				
		LEU	TRP	ASP	TYR	ASN	TRP				
Friedelin	2	02	31	49	52	67	70				
		LEU	TRP	ASP	TYR	ASN	TRP				
Rutin	2	02	31	49	52	67	70				
		LEU	TRP	ASP	TYR	ASN	TRP				
Quercetin	1	01	02	31	52	67	70				
		SER	LEU	TRP	TYR	ASN	TRP				
Beta-sitosterol	2	02	31	49	52	67	70				
		LEU	TRP	ASP	TYR	ASN	TRP				

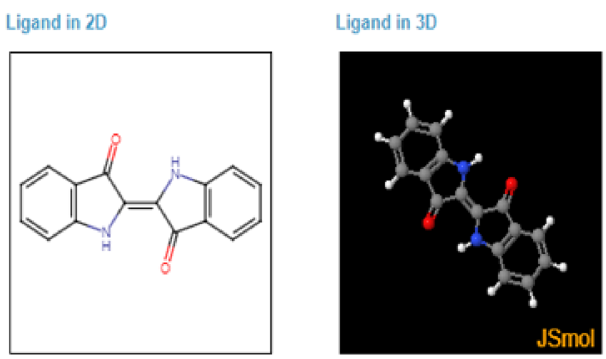

2.1 Indigotin

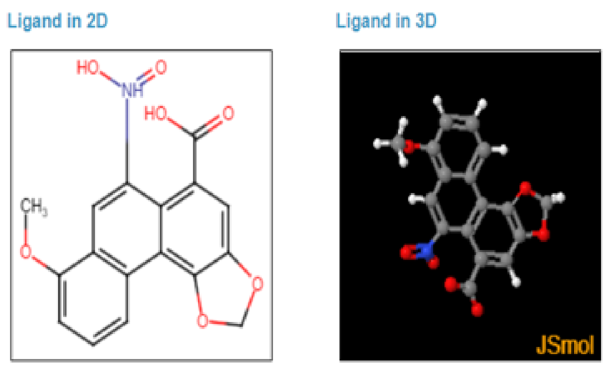

2.2 Aristolochic acid

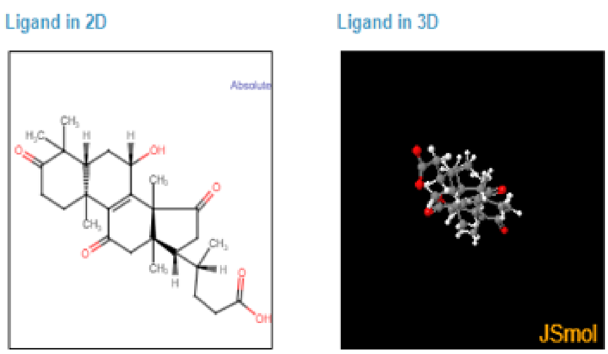

2.3 Lucidenic acid

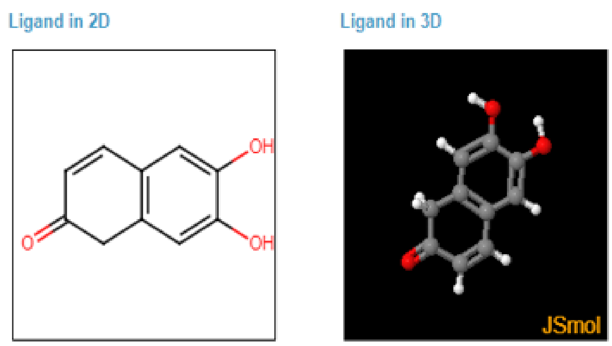

2.4 Esculetin

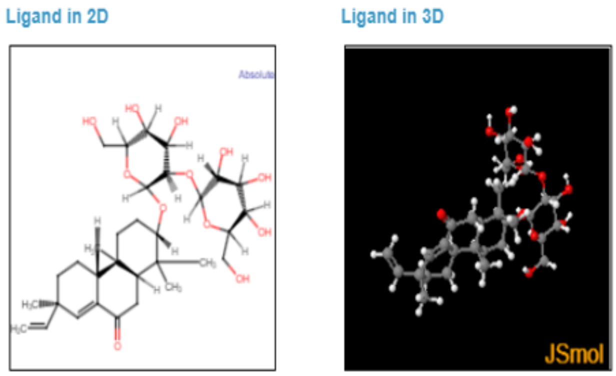

2.5 Leucasperoside B

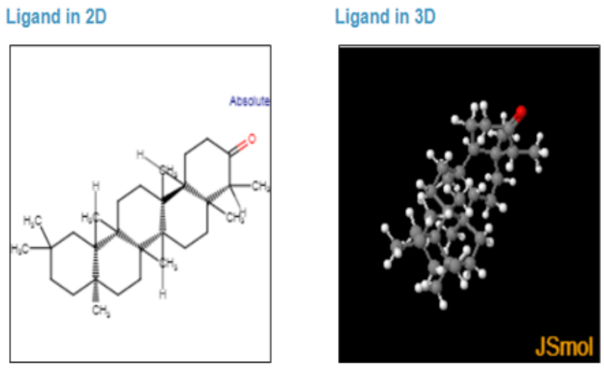

2.6 Friedelin

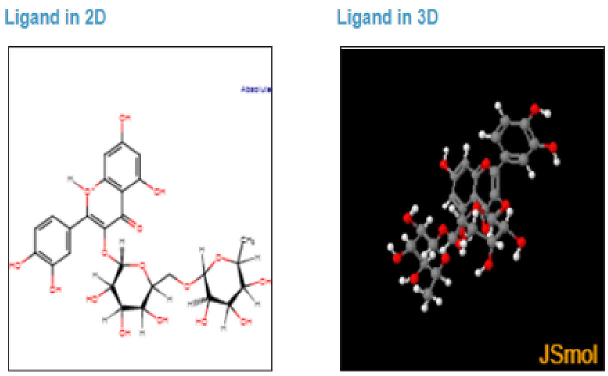

2.7 Rutin

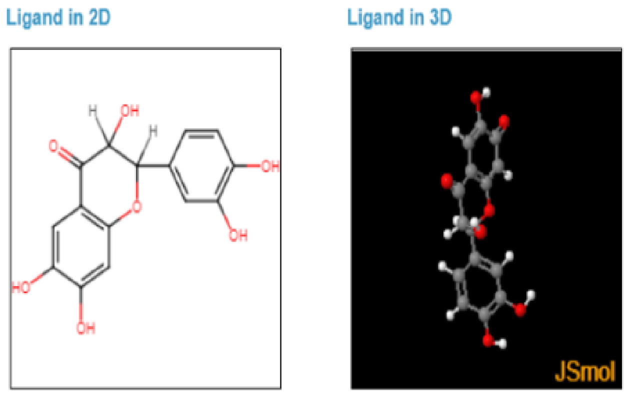

2.8 Quercetin

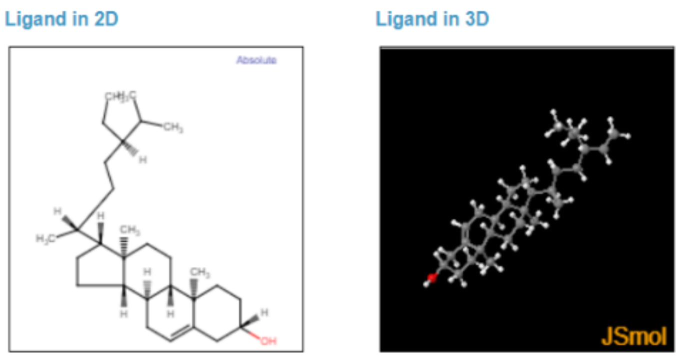

2.9 Beta-sitosterol

Figure 2: 2D and 3D Structure of Selected Ligands

3.1.Indigotin with Phospholipases A2 (PDB)2QOG

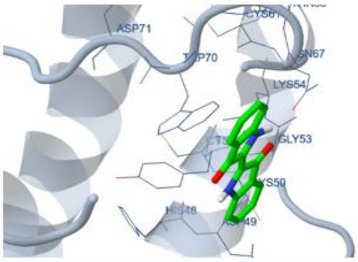

3.2.Aristolochic acid with Phospholipases A2 (PDB)2QOG

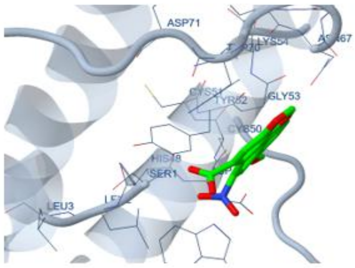

3.3.Lucidenic acid with Phospholipases A2 (PDB)2QOG

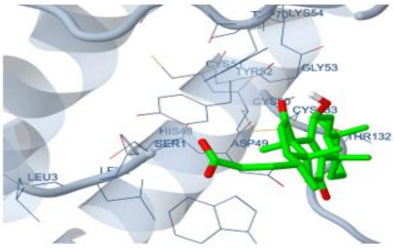

3.4.Esculetin with Phospholipases A2 (PDB)2QOG

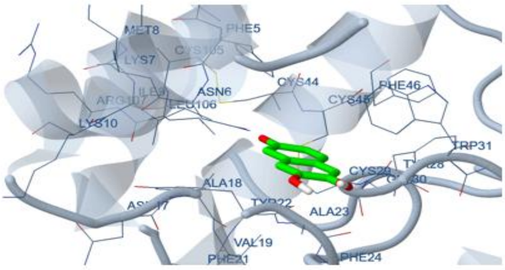

3.5.Leucasperoside B with Phospholipases A2 (PDB)2QOG

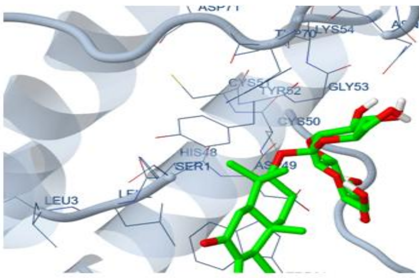

3.6.Friedelin with Phospholipases A2 (PDB)2QOG

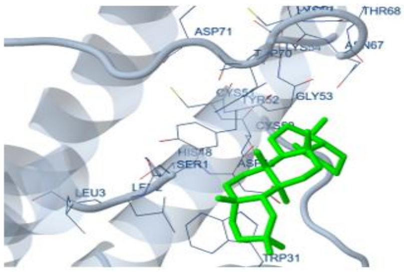

3.7.Rutin with Phospholipases A2 (PDB)2QOG

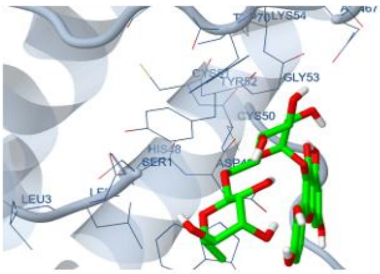

3.8.Quercetin with Phospholipases A2 (PDB)2QOG

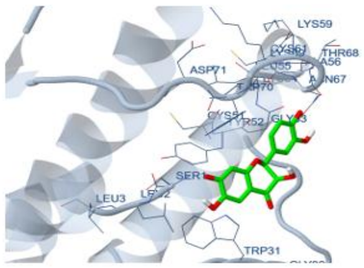

3.9.β-sitosterol with Phospholipases A2 (PDB)2QOG

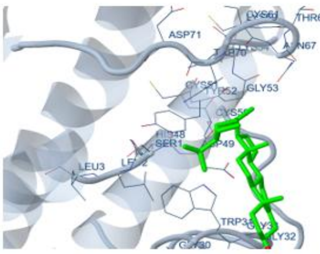

Figure 3: The docking pose of the ligands with the target receptor phospholipase A2 [PDB: 2QOG]

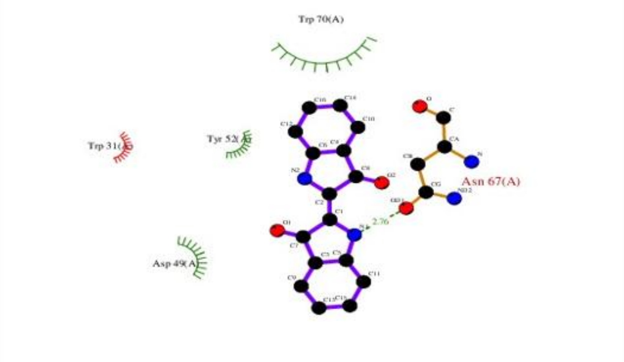

4.1.Indigotin

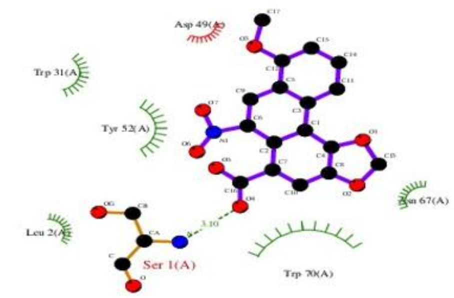

4.2.Aristolochic acid

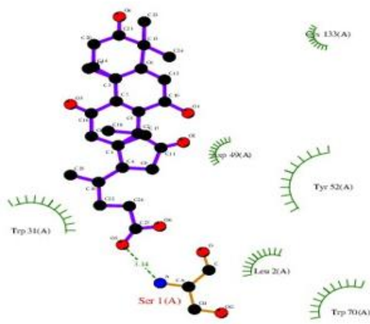

4.3.Lucidenic acid

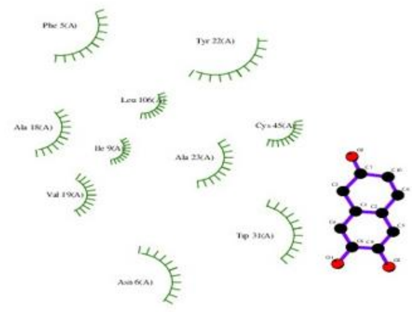

4.4.Esculetin

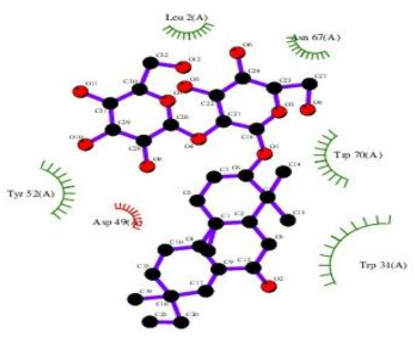

4.5.Leucasperoside B

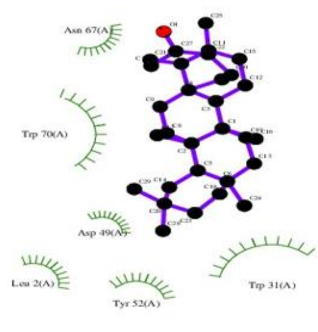

4.6.Friedelin

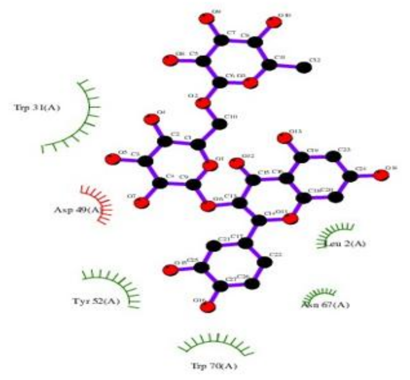

4.7.Rutin

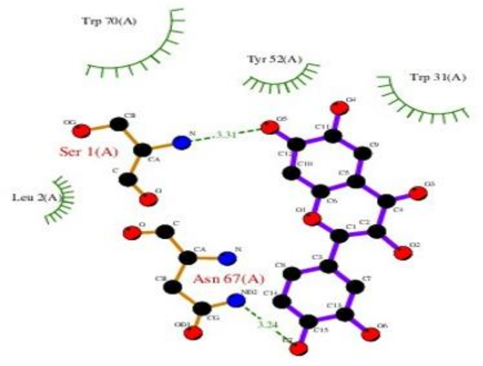

4.8.Quercetin

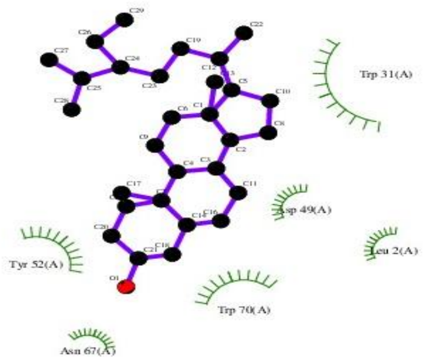

4.9.β-sitosterol

Figure 4: 2D interaction plot analysis of the ligands with the target receptor Phospholipase A2 [PDB: 2QOG]

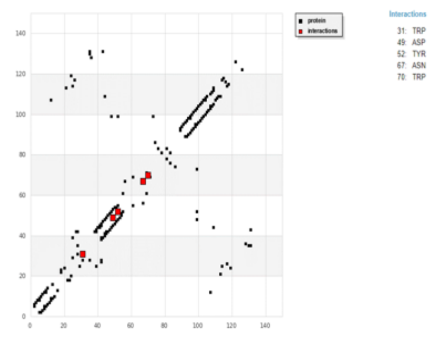

5.1.Indigotin

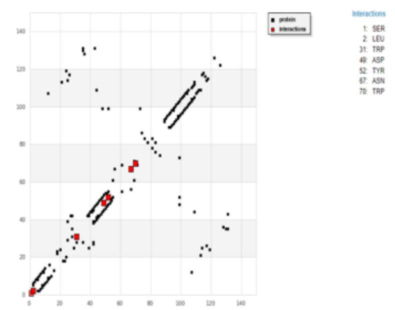

5.2.Aristolochic acid

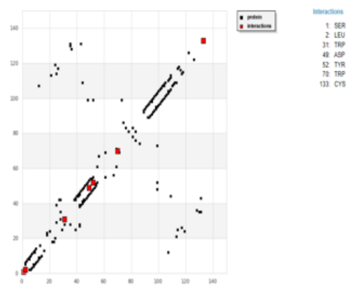

5.3.Lucidenic acid

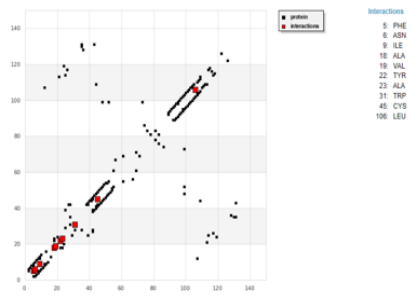

5.4.Esculetin

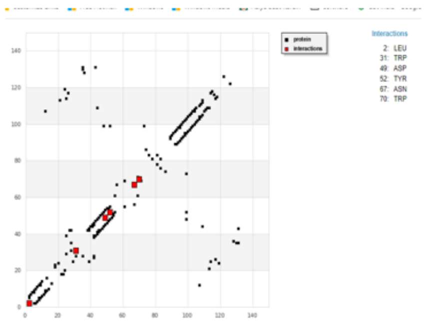

5.5.Leucasperoside B

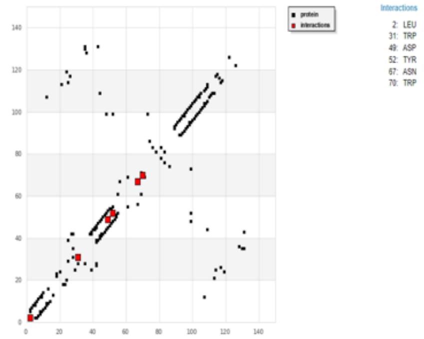

5.6.Friedelin

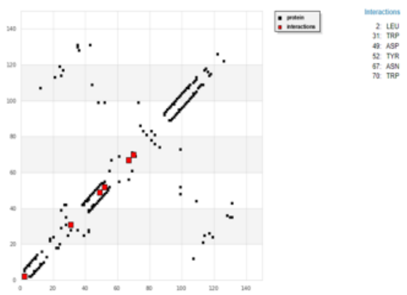

5.7.Rutin

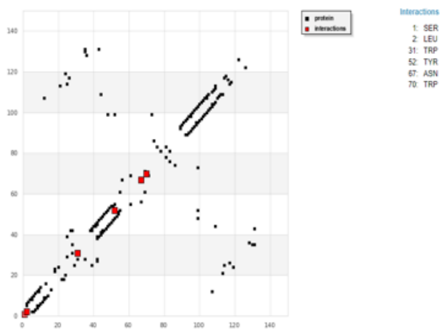

5.8.Quercetin

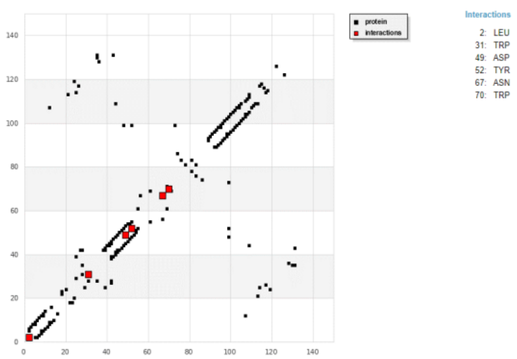

5.9.β-sitosterol

Figure 5: Hydrogen bond interactions along with core amino acid analysis of the ligands with the target receptor Phospholipase A2 [PDB: 2QOG]

DISCUSSION

The current *in silico* study identified Quercetin as the top candidate against snake venom secretory phospholipase A_2 ($sPLA_2$). It has a binding energy of −7.02 kcal/mol and directly interacts with the catalytic residue Tyr52. This finding matches previous work by Cotrim *et al.*, who showed that quercetin inhibited the enzymatic activity and various pharmacological effects of Crotalus durissus terrificus $sPLA_2$. These effects include a roughly 40% reduction in platelet aggregation and myotoxicity. Their molecular docking also showed hydrogen-bonded, polar, and hydrophobic interactions, indicating that similar flavonoids could bind to $sPLA_2$ [37]. The well-known oral bioavailability and high gastrointestinal absorption of quercetin in humans further support its potential, as reviewed by Almeida *et al* [38]. Additionally, Lesjak *et al.* highlighted the compound's antioxidant and anti-inflammatory properties, expanding its use beyond just blocking the enzyme [39].

Lucidenic acid emerged as a strong secondary candidate with a binding energy of −7.57 kcal/mol, engaging critical residues Asp49 and Tyr52. However, the pharmacokinetics and bioavailability of lucidenic acids have not been studied, which is vital for designing formulations and determining dosages. This is particularly important since the structurally related ganoderic acid A had an oral bioavailability as low as 8.68% in rat models. This gap needs to be filled before considering lucidenic acid as a clinical candidate [40].

Friedelin and Beta-sitosterol, despite slightly exceeding Egan's lipophilicity limits, showed strong binding affinities of −7.53 and −7.69 kcal/mol, respectively. They are proposed as candidates for topical anti-venom formulations aimed at treating local tissue necrosis. Evidence supports this, as β-sitosterol showed anti-inflammatory activity and good skin absorption, demonstrating the highest uptake among tested phytosterols, indicating its potential for developing topical anti-inflammatory treatments [41].

Indigotin showed unique blood-brain barrier permeability and a favorable QEDw score, but it had the weakest binding affinity at −5.62 kcal/mol. Although indigo significantly reduced carrageenan-induced paw swelling and acetic acid-induced vascular permeability in mice via the IKKβ/IκB/NF-κB pathway, [42]. its weak interaction with the $sPLA_2$ active site requires optimization of the structure before it can be considered a primary candidate against PLA_2.

CONCLUSION

This study presents the first systematic *in silico* analysis of nine Siddha medicinal plant compounds targeting snake venom Phospholipase A_2, utilizing drug-likeness, ADMET, and molecular docking approaches. Most compounds demonstrated favourable binding within the active site of PLA_2, specifically interacting with the key catalytic residues Asp49 and Tyr52, which are critical for enzymatic activity. These computational findings provide a rationale for the traditional use of these Siddha plants in snakebite treatments and underscore their potential for further experimental investigation. The results contribute to the growing body of evidence supporting plant-based inhibitors of snake venom enzymes and may inform the development of accessible and affordable adjunct therapies to complement existing antivenom treatments, particularly in regions where snakebites remain a significant public health concern.

Acknowledgements

The authors acknowledge the use of computational tools and databases for this research.

Conflict of interest

The authors declared no conflict of interest.

Financial Support

None declared.

ORCID ID

Chenthamarai Selvi Ganesan: https://orcid.org/0009-0001-8253-3315
Shanmugam Muthu: https://orcid.org/0009-0001-6184-9759

REFERENCES

1. Gutierrez JM, Calvete JJ, Habib AG, Harrison RA, Williams DJ, Warrell DA. Snakebite envenoming. Nat Rev Dis Primers. 2017;3:17063.
2. Kini RM. Excitement ahead: structure, function and mechanism of snake venom phospholipase A2 enzymes. Toxicon. 2003;42(8):827-40.
3. Dennis EA. The growing phospholipase A2 superfamily of signal transduction enzymes. Trends Biochem Sci. 1997;22(1):1-2.
4. Arni RK, Ward RJ. Phospholipase A2–a structural review. Toxicon. 1996;34(8):827-41.
5. Williams DJ, Habib AG, Warrell DA. Clinical studies of the effectiveness and safety of antivenoms. Toxicon. 2018;150:1-10.
6. Mors WB, Nascimento MC, Pereira BM, Pereira NA. Plant natural products active against snake bite – the molecular approach. Phytochemistry. 2000;55(6):627-42.
7. Gomes A, Das R, Sarkhel S, Mishra R, Mukherjee S, Bhattacharya S, *et al.* Herbs and herbal constituents active against snake bite. Indian J Exp Biol. 2010;48(9):865-78.
8. Manonmani S, Madhavan R, Shanmugapriya P, Manjari V, Murugesan S, Banumathi V. A review of beneficial effects of Siddha medicinal herbs on snake bite. Int J Curr Res Biol Med. 2016;1(7):27–35.
9. Borges MH, Alves DL, Raslan DS, Piló-Veloso D, Rodrigues VM, Homsi-Brandeburgo MI, *et al.* Neutralizing properties of *Musa paradisiaca* L. (Musaceae) juice on phospholipase A2, myotoxic, hemorrhagic and lethal activities of crotalidae venoms. J Ethnopharmacol. 2005;98(1–2):21-9.
10. Alam MI. Inhibition of toxic effects of viper and cobra venom by Indian medicinal plants. Pharmacology & Pharmacy. 2014;5(8):828-37.
11. Chandrakala AN, Reddy AH, Nageswari G, Sri DV, Begum SS, Venkatappa B. Anti venom and immunomodulatory functions of *Corallocarpus epigaeus* L. Int J Pharma Bio Sci. 2013;4(3):12-8.
12. Ethnobotanical records: traditional use of *Corallocarpus epigaeus* for snake bite. Front Pharmacol. 2022;13:903832.
13. Phytochemical studies show bioactive compounds in C. epigaeus that may act on venom proteins. Res Rep. 2022;1:1-5.
14. Balasubramani A, Ramasamy S, Mani KV. *Indigofera tinctoria* Linn. root bark paste: a potent antidote in treating various toxicity. Indian J Nat Sci. 2025;16(91):1-5.
15. Alam MI, Auddy B, Gomes A. Viper venom neutralization by Indian medicinal plant (*Hemidesmus indicus* and *Pluchea indica*) root extracts. Phytother Res. 1996;10(1):58-61.
16. Morris GM, Huey R, Lindstrom W, Sanner MF, Belew RK, Goodsell DS, *et al.* AutoDock4 and AutoDockTools4: automated docking with selective receptor flexibility. J Comput Chem. 2009;30(16):2785-91.
17. Xiao H, Pan H, Liao K, Yang M, Huang C. Snake venom PLA2, a promising target for broad-spectrum antivenom drug development. Biomed Res Int. 2017;2017:6592820.
18. Sivaraman D, Pradeep PS. Exploration of bioflavonoids targeting dengue virus NS5 RNA-dependent RNA polymerase: *in silico* molecular docking approach. J Appl Pharm Sci. 2020;10(5):16-22.

19. Sivaraman D. Study on exploration and evaluation of novel phytocomponents targeting DPP-4 enzyme in the treatment of type-1 diabetes by molecular docking analysis. Int J Sci Eng Res. 2017;8(6):947-68.
20. Sivaraman D, Pradeep PS, Manoharan SS, Jeyabalan S, Vijayarangan DR. Revealing anti-fungal potential of plant-derived bioactive therapeutics in targeting secreted aspartyl proteinase (SAP) of *Candida albicans*: a molecular dynamics approach. J Biomol Struct Dyn. 2024;42(2):710-24.
21. Morris GM, Goodsell DS, Halliday RS, Huey R, Hart WE, Belew RK, *et al*. Automated docking using a Lamarckian genetic algorithm and an empirical binding free energy function. J Comput Chem. 1998;19(14):1639-62.
22. Lipinski CA, Lombardo F, Dominy BW, Feeney PJ. Experimental and computational approaches to estimate solubility and permeability in drug discovery and development settings. Adv Drug Deliv Rev. 2001;46(1-3):3-26.
23. Daina A, Michielin O, Zoete V. SwissADME: a free web tool to evaluate pharmacokinetics, drug-likeness and medicinal chemistry friendliness of small molecules. Sci Rep. 2017;7:42717;1-13.
24. Pires DE, Blundell TL, Ascher DB. pkCSM: predicting small-molecule pharmacokinetic and toxicity properties using graph-based signatures. J Med Chem. 2015;58(9):4066-72.
25. Sajid M. Phytochemistry and pharmacology of genus Indigofera: a review. Rec Nat Prod. 2018;12(1):1-13.
26. Mohamed MS, Idriss MT, Khedr AI, Abd AlGadir H, Takeshita S, Shah MM, *et al*. Activity of Aristolochia bracteolata against *Moraxella catarrhalis*. Int J Bacteriol. 2014;2014:481686;1-6.
27. Songserm P, Klanrit P, Phetcharaburanin J, Thanonkeo P, Apiraksakorn J, Phomphrai K, *et al*. Antioxidant and anticancer potential of bioactive compounds from *Rhinacanthus nasutus* cell suspension culture. Plants (Basel). 2022;11(15):1994.
28. Prajapati MS, Patel JB, Modi K, Shah MB. *Leucas aspera*: a review. Pharmacogn Rev. 2010;4(7):85-7.
29. Sati H, Sati B. Phytochemical and pharmacological potential of *Aristolochia indica*: a review. Res J Pharm Biol Chem Sci. 2011;2(4):648-54.
30. Aneja V. Phyto-pharmacology of *Hemidesmus indicus*. Pharmacogn Rev. 2008;2(3):1-12.
31. Zafar M. *Musa paradisiaca* L. and *Musa sapientum* L.: a phytochemical and pharmacological review. J Appl Pharm Sci. 2011;1(5):14-20.
32. Karthic VM. *In-silico* molecular docking analysis of potential phytotherapeutics from the medicinal herb *Corallocarpus epigaeus* for treating urticarial. Int J Trans Res Ind Med. 2019;1(2):05-12.
33. Ghose AK, Viswanadhan VN, Wendoloski JJ. A knowledge-based approach in designing combinatorial or medicinal chemistry libraries for drug discovery. 1. A qualitative and quantitative characterization of known drug databases. J Comb Chem. 1999;1(1):55-68.
34. Veber DF, Johnson SR, Cheng HY, Smith BR, Ward KW, Kopple KD. Molecular properties that influence the oral bioavailability of drug candidates. J Med Chem. 2002;45(12):2615-23.
35. Egan WJ, Merz KM Jr, Baldwin JJ. Prediction of drug absorption using multivariate statistics. J Med Chem. 2000;43(21):3867-77.
36. Mohamed Tap F, Abd Majid FA, Ismail HF, Wong TS, Shameli K, Miyake M, *et al*. *In silico* and *in vitro* studies of phytochemical inhibition of phospholipase A2. Molecules. 2018;23(1):73.
37. Cotrim CA, de Oliveira SC, Diz Filho EB, Fonseca FV, Baldissera L Jr, Antunes E, *et al*. Quercetin as an inhibitor of snake venom secretory phospholipase A2. Chem Biol Interact. 2011;189(1-2):9-16.
38. Almeida AF, Borge GIA, Piskula M, Tudose A, Tudoreanu L, Valentová K, *et al*. Bioavailability of quercetin in humans with a focus on interindividual variation. Compr Rev Food Sci Food Saf. 2018;17(3):714-31.
39. Lesjak M, Beara I, Simin N, Pintać D, Majkić T, Bekvalac K, *et al*. Antioxidant and anti-inflammatory activities of quercetin and its derivatives. J Funct Foods. 2018;40:68-75.
40. Zheng C, Rangsinth P, Shiu PH, Wang W, Li R, Li J, Kwan YW, Leung GP. A review on the sources, structures, and pharmacological activities of lucidenic acids. Molecules. 2023;28(4):1756.
41. Chang ZY, Chen CW, Tsai MJ, Chen CC, Alshetaili A, Hsiao YT, Fang JY. The elucidation of structure–activity and structure-permeation relationships for the cutaneous delivery of phytosterols to attenuate psoriasiform inflammation. Int Immunopharmacol. 2023;119:110202.
42. Liu N, Zhang G, Niu Y, Wang Q, Zheng J, Yang J, *et al.* Anti-inflammatory and analgesic activities of indigo through regulating the IKKβ/IκB/NF-κB pathway in mice. Food Funct. 2020;11(10):8537-48.

HOW TO CITE THIS ARTICLE

Ganesan CS, Muthu S. *In silico* molecular docking evaluation of phytochemicals from Siddha medicinal plants as potential inhibitors of snake venom phospholipase A_2. J Phytopharmacol 2026; 15(2):164-175. doi: 10.31254/phyto.2026.15207